# Output Characteristics of RF-Modulated Laser Diodes

T. Wicht, S. Schuster, H. Haug, Joachim Sacher, M. Hofmann, Wolfgang Elsässer, and Ernst O. Göbel

*Abstract*—**We examine theoretically and experimentally the output characteristics of periodically current-modulated laser diodes with and without an external resonator. The total emitted intensity per modulation period shows, as a function of the dc part of the pump current, a characteristic saturation behavior (kink) each time before the number of emitted pulses per modulation period increases.**

## I. Introduction

SEMICONDUCTOR lasers can be employed as compact, reliable sources for the generation of short laser light pulses. Gain switching and active mode locking are the most common techniques to obtain stable pulse trains. In gain switching experiments, a dc pump current keeps the diode below or close to threshold, and a superimposed modulated pump current drives the laser diode periodically above the threshold [1]–[3]. Placing a laser diode with antireflection coating on one of its endfaces in an external resonator and modulating the diode with a frequency close to the roundtrip time introduces mode locking [4]–[6]. With this technique, the pulses can be shortened further, and pulse-to-pulse time jitter can be reduced.

Chaotic motion or period doubling sequences [7]–[10] may occur for modulation frequencies comparable to the intrinsic relaxation oscillation frequency of the laser diode. For much smaller modulation frequencies, no irregular behavior is expected if the diode is not self-pulsing; nevertheless, in the gain-switched as well as in the mode-locked case, one can obtain multiple pulses per modulation period [11]–[13]. Multiple spiking can be caused by reflections at the diodes' endfaces if the optical pulses are shorter than the diode roundtrip time [14], [15]; but for gain-switched diodes, spiking is in general a manifestation of the relaxation oscillation frequency [7], [8], [16]. Thus, more and more pulses per modulation period are obtained when the dc part of the current is increased keeping the sinusoidal current modulation constant [11].

We consider in this paper the light–current output characteristics and the time-resolved light output of a gain-switched semiconductor laser with and without an external resonator. We show theoretically and experimentally that nonlinear output characteristics can be obtained without introducing an intensity-dependent gain saturation. A saturation kink in the light–current characteristics occurs each time the number of pulses emitted per modulated period increases by one. This nonlinear behavior of the output characteristics for a mode-locked semiconductor laser has been reported previously [17], but has been assumed to be due to nonlinear gain saturation. We will show that a very similar behavior for the light–current characteristics is obtained for the mode-locked laser in an external cavity and the solitary laser, even though the mechanisms which yield the multiple pulse emission in both cases are rather different.

Manuscript received October 12, 1990; revised February 15, 1991. This work was supported by the Deutsche Forschungsgemeinschaft under Sonderforschungsbereich 185.

T. Wicht, S. Schuster, and H. Haug are with the Institut für Theoretische Physik der J. W. Goethe Universität, D 6000 Frankfurt am Main, Germany.

J. Sacher, M. Hofmann, W. Elsässer, and E. O. Göbel are with the Fachbereich Physik der Philipps-Universität, D 3350 Marburg, F. R. Germany.

IEEE Log 9100206.

## II. Gain Modulation in an External Resonator Configuration

We first consider an experimental arrangement as usually employed for active mode locking of diode lasers: one facet of the laser diode is antireflection coated and the diode is coupled to an external mirror using a microscope objective. The pump current of the laser is then modulated with a frequency close to the roundtrip frequency of the external cavity.

We now investigate the rate equations for the intensity of the traveling lightwaves and the carrier density. The light intensities in the diode (measured in terms of the photon density) of the forward and backward running wave $I^+$ and $I^-$ obey the equations

$$\left(\frac{\partial}{\partial t} \pm v_g \frac{\partial}{\partial z} - (g(N(t)) - v_g \alpha_{\text{int}})\right) I^{\pm}(z, t) = \beta N(t) \tag{1}$$

where $v_g$ is the group velocity, $g(N(t))$ is the optical net gain per unit time which depends on the electron-hole plasma density $N$, and $\alpha_{\text{int}}$ is the internal loss per unit length. $\beta$ is the fraction of spontaneous emission into the lasing modes. The time is measured in units of the spontaneous recombination time $T$.

The density of the thermal electron-hole plasma in the active region of the diode is assumed to be spatially homogeneous. This assumption is valid if the light pulse length is large compared to the length of the diode, and if the wavelength is short compared to the diffused length. Both assumptions hold for the experiments analyzed in this paper. The rate equation for the plasma density is given by

$$\dot{N}(t) = j(t) - N(t) - g(N(t)) \langle I(t) \rangle_z \quad (2)$$

where $j(t)$ is the injection rate of the carrier density. This injection rate is modulated periodically:

$$j(t) = j_0 + j_m \sin \omega_m t. \quad (3)$$

The constant injection rate $j_0$ corresponds to the dc current and is choosen to be below the laser threshold. We consider (1)–(3) for a small detuning $\delta$ between the total round-trip time in the resonator $\tau_R$ and the modulation period $\tau_m$, i.e.,

$$\delta = \tau_R - \tau_m << \tau_R.$$

An integration of (1) yields the difference equation

$$I^{\pm}(z \pm \Delta z, t + \Delta t) = I^{\pm}(z, t)\, S(t + \Delta t, t) + \beta \int_t^{t+\Delta t} dt'\, N(t')\, S(t + \Delta t, t')$$

where

$$S(t, t') = \exp\left[\int_{t'}^{t} dt''\, [g(N(t'')) - v_g \alpha_{\text{int}}]\right] \quad (4)$$

with $\Delta z = v_g \Delta t$. The boundary conditions at the endfaces of the laser diode are

$$I^{+}(0, t) = R_1 I^{-}(0, t) \quad (5)$$

$$I^{-}(L, t) = R_2 I^{+}(L, t - \tau_R + \tau_i). \quad (6)$$

Here, $\tau_i$ is the round-trip time in the laser diode. $L$ is the length of the diode, and $R_1$ and $R_2$ are the reflection coefficients of the uncoated diode endface and of the external mirror, respectively. We assume that the main effect introduced by the intracavity optical elements is a change in the optical length of the cavity and can be regarded by an effective $\tau_R$.

Under the condition

$$\left|\Delta\tau \frac{\dot{N}}{N}\right| << 1 \quad (7)$$

we can compute (4)–(6) together with (2) on a space–time lattice of width $\Delta\tau = \tau_i/2n$. For high pulse intensities, the change of the carrier density is dominated by stimulated emission, so that (7) becomes a condition for the maximum allowed pulse intensity.

We take the gain function in a linearized form

$$g(N(t)) = A(N(t) - N_t) \quad (8)$$

where $A = \partial g/\partial N$, and $N_t$ is the transparency density. Note that no saturation is taken into account. The average intensity is calculated as

$$\langle I \rangle_z = \frac{\exp\left[(g_{\text{eff}}(N(t)))\Delta\tau\right] - 1}{g_{\text{eff}}(N(t))\tau_i/2} \sum_{k=1}^{n} (I_k^{+} + I_{k+1}^{-}) + \frac{2\beta N}{g_{\text{eff}}(N(t))} \left(\frac{\exp\left[g_{\text{eff}}(N(t))\Delta\tau\right] - 1}{g_{\text{eff}}(N(t))\Delta\tau} - 1\right)$$

with the effective gain

$$g_{\text{eff}}(N(t)) = g(N(t)) - v_g \alpha_{\text{int}} \quad (9)$$

where $I_k^{\pm}$ are the intensities on the $k$th place of the lattice. The contribution of the spontaneous emission is important in numerical calculations to achieve a fast convergence with decreasing lattice width.

In Fig. 1, the output characteristics are shown for three different modulation frequencies. For reasons discussed below, the effective round-trip time is taken for all curves to be $\tau_R = 3.3$ ns corresponding to a cavity resonance frequency of 300 MHz. The other parameters used in the calculations are listed in Table I. The calculated output characteristics are highly nonlinear for $\delta > 0$ and show pronounced kinks. We also have calculated the time-resolved emission output and plotted the result in Fig. 2 for three different dc currents as marked in the characteristics (Fig. 1) by a, b, and c. In addition, we show in Fig. 2 the temporal variation of the electron-hole density. The threshold carrier density is indicated by the dotted line. Comparison of Figs. 2 and 1 reveals that the number of pulses emitted in one modulation period increases by one whenever a saturation structure appears. Thus, the kinks in the output characteristics are connected to multiple-pulse emission and can be explained as follows. When the carrier density in the diode exceeds the threshold value, a first light pulse is emitted. After one round-trip time $\tau_R$, the pulse reenters the diode again, now delayed with respect to the modulation, and bleaches the gain bringing the carrier density back below the threshold value. For a sufficiently high dc current, the density may exceed the threshold density a second time during the pump pulse and a next light pulse will be emitted. The current required to bring the density again above threshold causes the saturation kink in the output characteristics. Only after the threshold of the second pulse per modulation period is reached does the total light intensity increase again strongly with the dc current. Further increase of the dc current may generate a third pulse with a corresponding structure in the output characteristics, and so on. Multiple pulse generation occurs only within a certain regime for positive values of the detuning $\delta$. For small positive detuning, the thresholds for multiple-pulse emission are reached for smaller increments of the dc current, but the corresponding structures in the output characteristics are correspondingly small. For negative detuning, the light pulse precedes the maximum of the modulated gain and occurs at the rising edge of the carrier density [18]. One always obtains one pulse per modulation period, and consistently no steps are obtained in the intensity–current relation. The detuning value at which the structures in the characteristics vanish can therefore be used to determine the tuned situation $\delta = 0$, and thus the effective roundtrip time in the cavity.

These theoretical predictions are in close agreement with experimental findings. In Figs. 3 and 4, we depict experimental results for the output characteristics and the time-resolved emission of the laser for an experimental

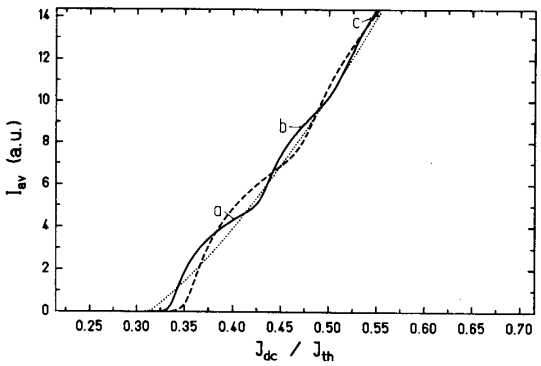


Fig. 1. Calculated light–current characteristics of the external cavity laser and three different modulation frequencies (· · · · 300 MHz, —— 301.2 MHz, - - - - 302.2 MHz).

TABLE I
PARAMETERS USED FOR THE CALCULATIONS

| Variable | Symbol | Value | Unit |
|---|---|---|---|
| Diode roundtrip time | $\tau_i$ | 6.6 | ps |
| Spontaneous lifetime | $T$ | 0.365 | ns |
| Gain coefficient | $A$ | $2.4 \cdot 10^{-6}$ | $cm^3\ s^{-1}$ |
| Carrier density for transparency | $N_t$ | $8.9 \cdot 10^{17}$ | $cm^{-3}$ |
| Spontaneous emission coupling | $\beta$ | $10^{-6}$ | |
| Mirror reflectivity | $R_1$, $R_2$ | 0.34 and 0.4 | |
| Group refractive index | $n_g$ | 4 | |
| Internal loss | $\alpha_{int}$ | 4.04 | $cm^{-1}$ |

configuration equivalent to the model used in the above calculations. We use a GaAs–AlGaAs index-guided double heterostructure laser diode (HLP 1400). The residual reflectivity of the antireflection coated endface of the diode was less than 0.1%. The external resonator length was $L$ = 50 cm corresponding to a resonator frequency $\tau_R^{-1}$ = 300 MHz. The effective reflectivity of the external mirror configuration including the coupling losses was 40%. In order to control the wavelength and spectral bandwidth, we also employ an intracavity etalon. The dc and the sinusoidal ac component of the injection current are superimposed in a bias tee. The time-averaged light output of the external cavity laser is detected by a slow Si PIN-photodiode, and the time-resolved output is analyzed with a synchroscan streak camera with a time resolution of 10 ps. The time-averaged light intensity of the modulated laser versus the dc current is depicted in Fig. 3 for three different modulation frequencies: 300, 301.2, and 302.2 MHz. As expected from our calculations, the light-current characteristics are linear without kinks for modulation frequencies of 300 MHz and below. For the two higher frequencies, the characteristics show saturation kinks followed by a steeper increase. The saturation kinks occur for larger increments of the dc current when the modulation frequency is increased. The time-resolved output of the RF-modulated external cavity laser is depicted in Fig. 4 for a modulation frequency of 301.2 MHz, and for three different currents marked by a, b, and c in

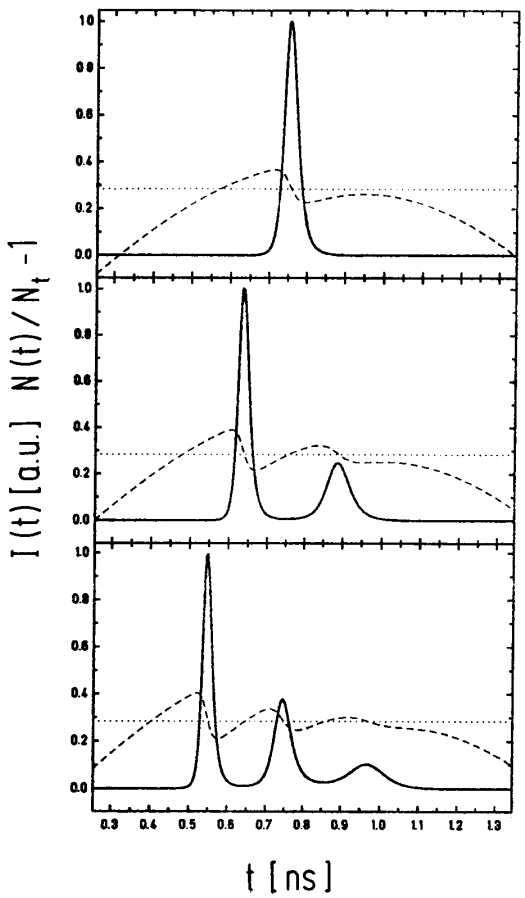


Fig. 2. Calculated intensity pulse pattern and plasma density patterns (dashed line) of the external cavity laser for the three dc currents marked as a, b, and c in Fig. 1 at the 301.2 MHz characteristics. The stationary threshold plasma density is given by the dotted line.

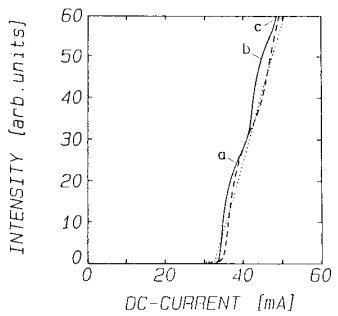


Fig. 3. Experimental light–current characteristics of the external cavity laser and three different modulation frequencies (· · · · 300 MHz, —— 301.2 MHz, - - - - 302.2 MHz).

Fig. 3. These streak camera traces reveal clearly that the number of pulses generated per modulation period increases, indeed, by one each time a kink in the output characteristics is passed, which can already be seen from the observed pulse patterns of Fig. 1 of [17]. Thus, we conclude that the nonlinear output characteristics of the

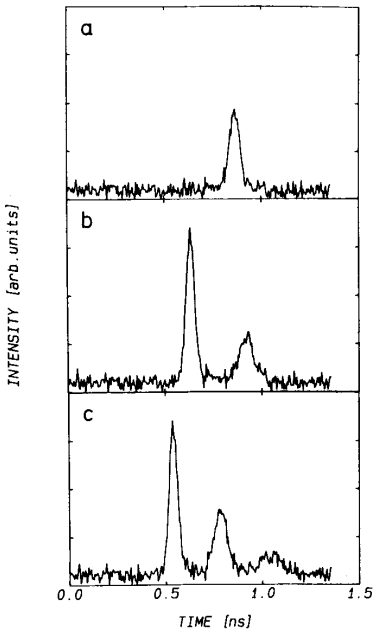


Fig. 4. Experimental pulse patterns of the external cavity laser for a modulation frequency of 301.2 MHz at three dc currents marked as a, b, and c in Fig. 3.

mode-locked semiconductor laser are due to multiple pulse generation. However, opposite to the analysis in [17], we do not have to introduce an intensity-dependent gain saturation.

In order to obtain a better understanding of the detuning dependence and to establish a connection with the solitary diode (without external cavity), we make the following considerations. For moderate pumping, (5) will be satisfied for a time step $\Delta\tau$ which equals the roundtrip time in the diode, i.e., $\Delta\tau = \tau_i$. Then the intensity equation reduces to a map for the intensity of the forward running field at the antireflection-coated diode surface.

$$I^+(L, t + \tau_R) = I^+(L, t) \exp\left[g_{\text{eff}}(N(t + \tau_R))\tau_i + \ln(R_1R_2)\right] + I^+_{sp}(t + \tau_R) \tag{10}$$

where $I^+_{sp}$ is the spontaneous emission amplified by the medium during one round-trip:

$$I^+_{sp}(t) = \frac{\beta N(t)}{g_{\text{eff}}(N(t))}\left(R_1 \exp\left[g_{\text{eff}}(N(t))\tau_i\right] + (1 - R_1)\exp\left[g_{\text{eff}}(N(t))\frac{\tau_i}{2}\right] - 1\right). \tag{11}$$

After the initial deviations have died out, the intensity and the carrier density are periodic with the period $\tau_m$ of the pump modulation. Therefore, the pulsed intensity obeys (10), in which the photon and the carrier densities are replaced by their stationary pulse values $I^+_s(t)$ and $N_s(t)$ (with $0 \le t < \tau_m$), respectively. The round-trip time $\tau_R$ is replaced by the detuning $\delta$.

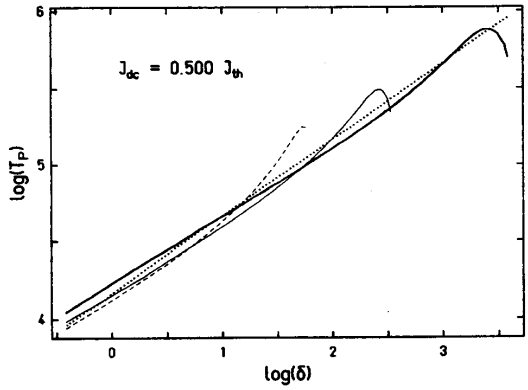


Fig. 5. Logarithmic plot of the time delay $T_p$ between the first and second pulse (full line) against the detuning $\delta$. The thin lines show the delays between second and third (——) and between the third and fourth pulse (----), respectively. The square-root approximation of (14) is given by the dotted line.

In the pulsed case, (10) can be approximated for small deviations of the gain from the threshold value and small detunings, i.e.,

$$\left|\delta\,\frac{\tau_i(AI\dot{N} + \dot{I}(g(N) - \tau_{ph}^{-1}))}{I}\right| \ll 1$$

by the differential equation

$$\dot{I}^+_s(t) = \frac{\tau_i}{\delta}\left(\left(g(N_s(t)) - \frac{1}{\tau_{ph}}\right)I^+_s(t) + \frac{I^+_{sp}(t)}{\tau_i}\right) \tag{12}$$

where $t$ runs over the time interval of one modulation period ($0 \le t < \tau_m$). A similar equation can be found for the averaged intensity in the diode. This equation is identical with the single-mode rate equation for the photon density of a solitary diode with the same gain and a photon lifetime $\tau_{ph}$ given by

$$\frac{1}{\tau_{ph}} = v_g\alpha_{\text{int}} - \frac{\ln(R_1R_2)}{\tau_i} \tag{13}$$

except for the prefactor $\tau_i/\delta$. Therefore, within our model, the actively mode-locked diode in an external cavity behaves like the solitary laser modulated at the same frequency and with a net gain enhanced by $\tau_i/\delta$. The relaxation oscillation frequency of such a laser is

$$\Omega_R \simeq \sqrt{\frac{\tau_i}{\delta}A(j - j_{th})}. \tag{14}$$

Since the multiple spiking of modulated solitary diodes is caused by relaxation oscillations, the pulse period in the mode-locked case should be proportional to the square root of $\delta$ according to (14). Fig. 5 shows for the first three multiple-pulse solutions that this relation is indeed fulfilled approximately, in spite of the fact that the modulation is by no means a small signal.

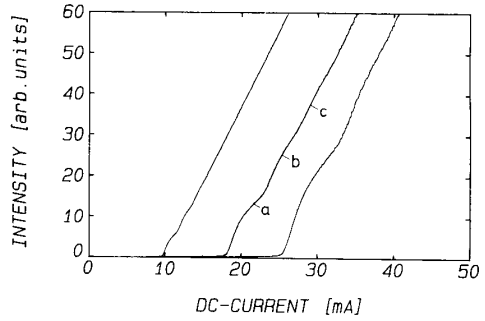


Fig. 6. Experimental light-current characteristics of the solitary laser diode for three different modulation frequencies 150.6 MHz (left), 301.2 MHz (middle), and 451.8 MHz (right).

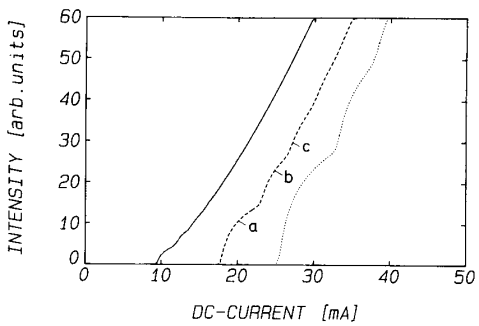


Fig. 8. Calculated light-current characteristics for the solitary laser for three different modulation frequencies and modulation amplitudes (—— 150.6 MHz and 45.5 mA, ---- 301.2 MHz and 41.5 mA, and · · · · 451.8 MHz and 38 mA).

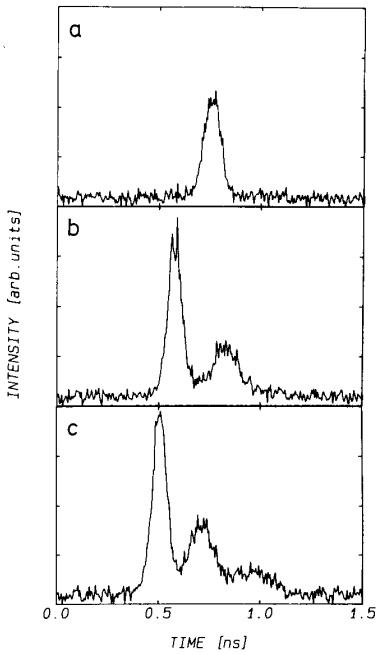


Fig. 7. Experimental pulse pattern of the solitary laser for a modulation frequency of 301.2 MHz and for three different dc currents marked as a, b, and c in Fig. 6.

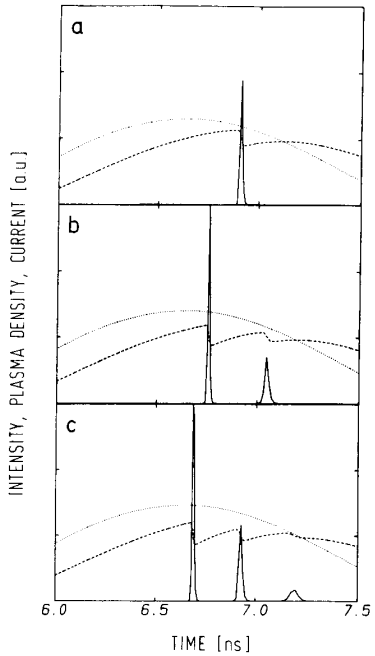


Fig. 9. Calculated patterns of the intensity pulses (——), the plasma density (----), and the injection current (· · · ·) of the solitary laser diode for three dc currents marked in Fig. 8 at the 301.2 MHz characteristics.

It is known that the frequency of the relaxation oscillations of a laser with a long external cavity is by orders of magnitude smaller than that of the solitary laser [19]. It is interesting to note that the relaxation oscillation frequency of the solitary diode reappears when active mode locking is applied.

Equation (12) becomes invalid for $|\delta| \ll \tau_i$, because shorter and more intense light pulses are obtained for decreasing detuning values, so that the condition (7) is violated. The shortest pulses are obtained for small but finite positive detuning. For negative detuning, the dynamics of the intensity is "time reversed" as compared to the solitary diode. This explains again the lack of multiple pulse solutions.

## III. Output Characteristics of the Modulated Solitary Diode

In order to check the predicted similarity between the mode-locked laser and the solitary laser [see (12)], we measured the characteristics of an uncoated CSP Laser (Hitachi HLP1400) without external cavity, again for three different modulation frequencies (150.6, 301.2, 451.8 MHz). The resulting characteristics obtained with a modulation amplitude which is 0.83 times the current threshold of the solitary diode are shown in Fig. 6. As expected from (12), the characteristics show the above-discussed structures due to multiple pulse emission. The measured time-resolved light intensities are shown in Fig.

7 for a modulation frequency of 301.2 MHz and three different dc currents, again indicated in Fig. 6 by a, b, and c. As in the case of external feedback, the saturation kinks are related to the occurrence of satellite pulses. Numerical simulations using rate equations of the type given in (2) and (12) are depicted in Figs. 8 and 9 showing the output characteristics and time-resolved output, respectively. The excellent agreement with the experimental results (Figs. 6 and 7) reveals that in fact already the rate equation model reproduces the saturation kinks without inclusion of a nonlinear gain. The inclusion of an explicit intensity-dependent gain saturation only results in an overall slight decrease of the slope of the intensity–current characteristics.

## IV. Conclusions

We have calculated and measured the light–current characteristics and the time-resolved output of an RF-current modulated semiconductor laser. We consider both cases: the laser with an external cavity used for active mode locking and the solitary laser diode. We demonstrate experimentally and theoretically the occurrence of saturation kinks in the light–current characteristics due to the onset of multiple pulse emission within one modulation period. This saturation behavior does not require a nonlinear gain coefficient. The formation of the satellite pulses which develop with increasing pumping into multiple pulses is solely due to the dynamics of the plasma density and the laser light intensity. In solitary lasers, the mechanism of their buildup is the relaxation oscillation.

## References


[1] I. H.-J. Klein, D. Bimberg, H. Beneking, J. Kuhl, and E. O. Göbel, "High peak power picosecond light pulses from a directly modulated semiconductor laser," *Appl. Phys. Lett.*, vol. 41, pp. 394–396, 1982.

[2] P. M. Downey, J. E. Bowers, R. S. Tucker, and E. Agyekum, "Picosecond dynamics of a gain-switched InGaAsP laser," *IEEE J. Quantum Electron.*, vol. QE-23, pp. 1039–1047, 1987.

[3] H. F. Liu, M. Fukazawa, and Y. Kawai, "Gain-switched picosecond pulse (< 10 ps) generation from 1.3 $\mu$m InGaAsP laser diodes," *IEEE J. Quantum Electron.*, vol. 25, pp. 1417–1424, 1989.

[4] P. T. Ho, L. A. Glasser, E. P. Ippen, and H. A. Haus, "Picosecond pulse generation with a CW GaAlAs laser diode," *Appl. Phys. Lett.*, vol. 33, pp. 241–242, 1978.

[5] J. Kuhl, M. Serenyi, and E. O. Göbel, "Bandwidth-limited picosecond pulse generation in an actively mode-locked GaAs laser with intracavity chirp compensation," *Opt. Lett.*, vol. 12, pp. 334–336, 1987.

[6] S. W. Corzine, J. E. Bowers, G. Przybylek, U. Koren, B. I. Miller, and C. E. Soccolich, "Actively mode-locked GaInAsP laser with subpicosecond output," *Appl. Phys. Lett.*, vol. 52, pp. 348–350, 1988.

[7] E. Hemery, L. Chusseau, and J. M. Lourtioz, "Dynamic behaviors of semiconductor lasers under strong sinusoidal current modulation: Modeling and experiments at 1.3 $\mu$m," *IEEE J. Quantum Electron.*, vol. 26, pp. 633–641, 1990.

[8] M. Tang and S. Wang, "Simulation studies of bifuraction and chaos in semiconductor lasers," *Appl. Phys. Lett.*, vol. 48, pp. 900–902, 1986.

[9] C. H. Lee, T. H. Yoon, and S. Y. Shin, "Period doubling and chaos in a directly modulated laser diode," *Appl. Phys. Lett.*, vol. 46, pp. 95–97, 1985.

[10] T. H. Yoon, C. H. Lee, and S. Y. Shin, "Perturbation analysis of bistability and period doubling in directly-modulated laser diodes," *IEEE J. Quantum Electron.*, vol. 25, pp. 1993–2000, 1989.

[11] H. Ito, H. Yokoyama, S. Murata, and H. Inaba, "Generation of picosecond optical pulses with highly RF-modulated AlGaAs-DH laser," *J. Quantum Electron.*, vol. QE-17, pp. 663–670, 1981.

[12] D. J. Bradley, M. B. Holbrook, and W. E. Sleat, "Bandwidth-limited picosecond pulses from an actively mode-locked GaAlAs diode laser," *J. Quantum Electron.*, vol. QE-17, pp. 658–662, 1981.

[13] K. Smith, J. M. Catherall, and G. H. C. New, "Comparison of experiment and theory in a synchronously mode-locked dye laser," *Opt. Commun.*, vol. 58, pp. 118–123, 1986.

[14] Y. Arakawa, T. Sogawa, M. Nishioka, M. Tanaka, and H. Sakaki, "Picosecond pulse generation in a quantum well laser by a gain switching method," *Appl. Phys. Lett.*, vol. 51, pp. 1295–1297, 1987.

[15] J. E. Bowers, P. A. Morton, A. Mar, and S. W. Corzine, "Actively mode-locked semiconductor lasers," *IEEE J. Quantum Electron.*, vol. 25, pp. 1426–1439, 1989.

[16] P. Paulus, R. Langenhoust, and D. Jäger, "Generation and optimum control of picosecond optical pulses from gain-switched semiconductor lasers," *IEEE J. Quantum Electron.*, vol. 24, pp. 1519–1523, 1988.

[17] M. Serenyi, E. O. Göbel, and J. Kuhl, "Inhomogeneous gain saturation in a mode-locked semiconductor laser," *Appl. Phys. Lett.*, vol. 53, pp. 169–171, 1988.

[18] S. Schuster, T. Wicht, and H. Haug, "Theory of the dynamical relaxation oscillations and of frequency locking in a synchronously pumped laser diode," *IEEE J. Quantum Electron.*, to be published.

[19] L. A. Glasser, "A linearized theory for the diode laser in an external cavity," *IEEE J. Quantum Electron.*, vol. QE-16, pp. 525–531, 1980.



**T. Wicht,** photograph and biography not available at the time of publication.

**S. Schuster,** photograph and biography not available at the time of publication.

**H. Haug,** photograph and biography not available at the time of publication.

**Joachim Sacher,** for a photograph and biography, see p. 379 of the March 1991 issue of this JOURNAL.

**M. Hofmann,** photograph and biography not available at the time of publication.

**Wolfgang Elsässer,** for a photograph and biography, see p. 379 of the March 1991 issue of this JOURNAL.

**Ernst O. Göbel,** for a photograph and biography, see p. 379 of the March 1991 issue of this JOURNAL.